Journal of Sustainable Development of Energy, Water and Environment Systems

http://www.sdewes.org/jsdewes

Year 2027, Volume 15, Issue 1, 1140773

Original Research Article

Prevention of Corrosion and Scale Formation Problems in Water Systems at 50 °C by Isobutylamide Derivatives of Ethylenediaminetetraacetic Acid

Teyyub A. Ismayilov*[1], Rahima M. Farhadova[1], Ismayil T. Ismayilov[1], Vagif M. Abbasov[1], Ayaz M. Mammadov[1,2,3], Sara M. Abbaszade[1], Elmir A. Manafov[4], Gunel T. Aghamaliyeva[1]

[1]Institute of Petrochemical Processes named after academician Y.H. Mammadaliyev of the Ministry of Science and Education of the Republic of Azerbaijan, AZ1025, Khojaly ave. 30, Baku, Azerbaijan

[2]Sumgait State University, Department of Chemistry, AZ5008, Baku Str. 1, Sumgait, Azerbaijan

[3]Azerbaijan University of Architecture and Construction, AZ1073, Ayna Sultanova Str. 5, Baku, Azerbaijan

[4]SEK International School Riyadh, 13315, Al Toq Str., Ar Rabi, Riyadh Saudi Arabia

e-mail: nkpi@nkpi.az, ayaz.mamedov@sdu.edu.az, ayaz.mammadov1@azmiu.edu.az, elmir.manafov@sek.sa

Cite as: Ismayilov, T. A., Farhadova, R. M., Ismayilov, I. T., Abbasov, V. M., Mammadov, A. M., Abbaszade, S. M., Manafov, E. A., Aghamaliyeva, G. T., Prevention of corrosion and scale formation problems in water systems at 50oC by isobutylamide derivatives of ethylenediaminetetraacetic acid, J.sustain. dev. energy water environ. syst., 15(1), 1140773, 2027, DOI: https://doi.org/10.13044/j.sdewes.d14.0773

ABSTRACT

The article identifies the minerals that cause salt deposition in various industrial sectors and provides information on reagents used to prevent salt deposition, emphasising a preference for reagents that are multifunctional, environmentally friendly and economically viable. Sodium and potassium salts of mono-, di-, and triisobutylamides of ethylenediaminetetraacetic acid were synthesised for testing as corrosion and scale-forming inhibitors in water systems at 50 °C. The structures of the synthesised compounds were confirmed by infrared spectroscopy, and their 10% solutions were prepared to determine the main physicochemical parameters. Inhibition of corrosion and salt deposition experiments were carried out at concentrations of 50, 100 and 150 mg L^{-1}. At 50 mg L^{-1}, the trisodium salt of the amide, synthesised from ethylenediaminetetraacetic acid and isobutylamine at a 1:1 molar ratio, exhibited the highest performance, providing 90% protection of the Steel-3 metal plates against corrosion and achieving 90% effectiveness against salt precipitation. Anti-corrosion and anti-scaling evaluations showed that increasing the salt concentration to 100 and 150 mg L^{-1} led to a proportional increase in effectiveness. Analysis of the results also indicated that the mono-, di-, and trisodium salts exhibited greater inhibitory activity than their corresponding potassium salts. In terms of activity, both the sodium and potassium salts followed the order: mono- < di- < tri-. It has been established that the inhibition mechanism of steel corrosion in the presence of synthesised salts is due to chemisorption, following the classical Langmuir adsorption isotherm. Additionally, calculations were performed to correlate the electronic properties of the inhibitors with their experimental performance, identifying the carboxylate and amide groups as the primary active centres for adsorption. The theoretical results, including frontier molecular energy-level analysis and electron-transfer fractions, provided a convincing explanation for the superior efficiency of the trisodium salt, consistent with the experimentally observed activity order of mono- < di- < tri-.

* Corresponding author

KEYWORDS

Water systems, Scale prevention, Corrosion inhibition, Ethylenediaminetetraacetic acid, Isobutylamide, Corrosion and salt-deposition reagent.

INTRODUCTION

Water, which is widely used in households, also plays a very important role in industry. The total volume of water consumed worldwide is increasing every day. The use of water in various industrial sectors, including mining, the transportation of raw materials through pipelines, heating and cooling systems, and the preparation of solutions, is well established. During the use of water in the mentioned systems, various processes, corrosion [1], salt deposition [2], biomass formation [3], may occur over time, leading to problems such as reduced liquid flow rates [4], disruption of technological regimes and operational efficiency, premature equipment failure, and consequently increased costs [5].

Mechanical and chemical cleaning of the system, which requires interrupting the technological process, should also be regarded as a factor contributing to increased operational costs [6]. Methods of removing scale and corrosion deposits generally include mechanical, hydrodynamic, chemical, and electro-pulse cleaning techniques. Among these, the use of chemical reagents [7] is the most widely used approach, as it is applied both to prevent the formation of corrosion and salt deposits [8], and to clean systems by dissolving existing deposits [9]. Thus, to avoid such problems, industrial enterprises apply corrosion and salt-deposition inhibitors to mitigate corrosion and scaling, and biocides to prevent biomass formation, as part of preventive measures.

Some reagents can perform multiple functions simultaneously, making their use more cost-effective. It is possible to cite examples that have demonstrated high effectiveness as carbon dioxide (CO_2) corrosion inhibitor and oil-collecting agent [10], a scale inhibitor and antibacterial agent [11], a corrosion inhibitor and biocide [12], and as a corrosion inhibitor in various aggressive environments [13].

Nowadays, increasing attention is being paid to developing multifunctional reagents, preferably synthesised from natural, renewable, and environmentally friendly raw materials. Paper [14] reviews recent research on the application of biomaterials as scale inhibitors in recirculating cooling water treatment systems. The study discusses various categories of environmentally friendly inhibitors, including proteins and amino acids, polysaccharides, plant extracts, microbial reagents, and microbiological products. In publication [15], the authors investigated a byproduct of white oil production and evaluated its potential as an inhibitor-bactericidal reagent. In research work [16], several novel green surfactants derived from cottonseed oil were synthesised and tested as corrosion inhibitors for mild steel in a CO_2-saturated 1% sodium chloride solution using potentiodynamic polarisation and linear polarisation resistance measurements at 50 °C. Similarly, article [17] investigated the adsorption behaviour and corrosion inhibition performance of a series of commercial fatty acid surfactants synthesised from vegetable oils, including sunflower, cottonseed, corn, and palm oils, on mild steel in CO_2-saturated brine at 50 °C. Research paper [18] reports the results of a study on green chemicals to address corrosion, scaling, and microbial growth in open recirculating cooling water systems. The proposed all-organic multicomponent inhibitor blend, consisting of citric acid, phosphonates (hydroxyethylidene diphosphonic acid), an acrylate copolymer, and isothiazolone, demonstrated an effective reduction in corrosion, scale deposition, and microbial growth under the tested conditions. Furthermore, the review article [19] provides a comprehensive overview of scale formation, various green scale inhibitors, their classifications, mechanisms of action, comparative performance, significance, and prospects, offering valuable insights for researchers and professionals in the oil and gas industry.

These reagents can be single-component or multicomponent compositions [20], [21], each performing an inhibitory function against one or more problems, such as corrosion, salt

deposition, biomass formation, and biocorrosion. In this case, the effective composition of a reagent is determined through laboratory experiments and subsequently applied in industry [22]. To ensure the successful application of the reagent, environmental technological parameters such as process temperature, flow rate, and the concentrations of various minerals in the water, as well as the material composition of equipment, should be considered [23].

The effectiveness of a salt-precipitation inhibitor is determined by the change in the total amount of calcium or salts in the environment. It is known that the main cause of scale formation is calcium carbonate ($CaCO_3$) present in water. In addition, minerals that contribute to salt precipitation include calcium sulphate, magnesium carbonate, magnesium sulphate, iron (II) carbonate, iron sulphide, and barium and strontium sulphates [24].

One effective method for treating mineral salt deposits is acid treatment of the medium. The first patent for this technology dates back to 1896 [25]. According to the patent, $CaCO_3$ reacts with hydrochloric acid during the acidification of the environment:

$$CaCO_3 + 2HCl = CaCl_2 + CO_2 + H_2O \quad (1)$$

Although it increased the efficiency of the system in which it was used fourfold, it did not gain widespread adoption due to the severe corrosion it caused in equipment and technological devices. However, subsequent research led to the development of composite reagents that simultaneously prevent corrosion, which are still widely used today.

The literature includes studies on the effectiveness of organic complex compounds [25], phosphorus compounds [26], [27], nitrogen compounds [28], [29], low-molecular-weight polymers based on polyacrylate and polymaleic anhydride [30], [31], and surfactants [32] against corrosion and salt deposition. As noted in the article [25], many experts consider acidic compositions prepared by adding chelating compounds to formulations highly effective against salt precipitation.

Zahraa and Falah [33] investigated the effectiveness of a corrosion inhibitor composition consisting of 100 ppm sodium benzoate, 60 ppm zinc sulfate, and ethylenediaminetetraacetic acid (EDTA) at concentrations of 10 and 20 ppm for carbon steel in saline environments at temperatures of 28, 33, and 38 °C. The results demonstrated a significant reduction in corrosion rates upon the addition of the inhibitors and revealed a synergistic effect among the components in mitigating corrosion. While the binary inhibitor system (sodium benzoate + zinc sulfate) provided moderate protection, with efficiencies of up to 78%, the addition of EDTA significantly enhanced the inhibition efficiency, indicating a strong synergistic interaction when all three components were present. The highest inhibition efficiency, exceeding 99%, was achieved with 20 ppm EDTA at 33 °C. It can be concluded that the combined action of anodic and cathodic inhibitors contributes to a reduction in the corrosion rate, while EDTA, acting as an anti-scaling agent, prevents the deposition of calcium and magnesium salts caused by temperature increases in heat exchangers.

Shaban *et al.* [34] and Brixi *et al.* [35] also investigated the combined effect of sodium benzoate and EDTA as corrosion inhibitors for carbon steel in chloride-containing solutions using electrochemical methods, with particular attention to the influence of temperature on inhibitor performance. The results demonstrated that the combined use of these inhibitors produced a synergistic effect, with inhibition efficiencies significantly higher than those achieved with each inhibitor alone. The findings further indicated the formation of a strong protective film on the steel surface, which effectively reduced the corrosion rate.

Chelate compounds widely used as solvents of salt precipitation include diethylenetriaminepentaacetic acid [36], ethylenediaminetetraacetic acid [37], hydroxyethylethylenediaminetriacetic acid [38], 1-hydroxyethane-1, 1-diphosphonic acid [39], and their derivatives. These compounds form complexes with metal ions, preventing their

precipitation as salts; do not participate in active chemical reactions; are low in toxicity, have low corrosive activity, and are easy to transport and store.

EDTA is a chelating ligand with a high affinity constant and is capable of forming stable metal-EDTA complexes [40, 41]. Since the chelation reaction is stoichiometric, one mole of EDTA, for example, can bind two moles of calcium ions (Ca^{2+}) [42]. Also, due to its ability to form complexes with charged metal ions [43], EDTA has been extensively studied as a corrosion inhibitor for metals in various environments [44], [45]. Complexation occurs through interactions between the vacant d-orbitals of the metal and the free or π-electrons of EDTA, leading to the formation of donor-acceptor surface complexes [45]. It has been found that several parameters influence the inhibition efficiency of EDTA, including pH, temperature, concentration, and the type of metal.

Azooz and Kamal [46] investigated the corrosion-inhibitory performance of disodium EDTA salt for mild steel in Red Sea water using weight-loss measurements and electrochemical techniques. Their results demonstrated that disodium EDTA salt acts as an effective corrosion inhibitor, achieving an inhibition efficiency of approximately 88% for mild steel in Red Sea water. Furthermore, the inhibition efficiency increased with increasing concentration of disodium EDTA and reaction temperature. In another study [47], Azooz tested the inhibitory effect of EDTA at very low concentrations on aluminium corrosion in 0.5 M hydrochloric acid solution. The calculated thermodynamic and adsorption parameters indicated that EDTA is chemisorbed onto the aluminium surface within this concentration range, forming a stable Al-EDTA complex with an inhibition efficiency of up to 89%.

The literature review indicates that EDTA and its derivatives are effective against both scale formation and corrosion, thereby performing multiple functions simultaneously. As mentioned earlier, the use of such reagents is considered economically advantageous, and research in this field is still under development.

The work presented in this article aimed to synthesise ethylenediaminetetraacetic acid mono-, di-, and tri-isobutyl amide derivatives and their corresponding sodium and potassium salts, to study the effectiveness of the synthesised compounds against corrosion and salt precipitation. Their activities as corrosion inhibitors in hydrogen sulphide environments and as bactericides against sulphate-reducing bacteria were evaluated [48], [49], yielding results that indicate the synthesised compounds may be regarded as multifunctional reagents.

MATERIALS AND METHODS

This section presents the materials and experimental procedures used in this study.

Synthesis Method of the Isobutylamide Derivatives of Ethylenediaminetetraacetic Acid

The synthesis of the sodium and potassium salts of mono-, di-, and triisobutylamides of ethylenediaminetetraacetic acid was carried out in two stages. In the first stage, mono-, di- and triisobutylamides of ethylenediaminetetraacetic acid were synthesised at temperatures of 120–150 °C via the reaction of EDTA with isobutylamine at molar ratios ranging from 1:1 to 1:3. In the second stage, the corresponding mono-, di-, and trisodium and potassium salts were obtained by reacting the synthesised amides with 20% aqueous sodium hydroxide NaOH or potassium hydroxide KOH solutions. Eq. (2) represents the synthesis reactions:

$$\begin{aligned}&(HOOCCH_2)_2NCH_2CH_2N(CH_2COOH)_2 + aNH_2CH_2CH(CH_3)CH_3 \longrightarrow \\ &(HOOCCH_2)_{4-a}(NCH_2CH_2N)(CH_2COO^- + NH_3CH_2CH(CH_3)CH_3)_a \longrightarrow \\ &(HOOCCH_2)_{4-a}(NCH_2CH_2N)(CH_2CONHCH_2CH(CH_3)CH_3)_a + aH_2O\end{aligned} \quad (2)$$

where a = 1–3; the compound $(HOOCCH_2)_{4-a}(NCH_2CH_2N)(CH_2CONHCH_2CH(CH_3)CH_3)_a$ is the general formula for the isobutylamides.

When the synthesised isobutylamides are exposed to an alkaline solution, they undergo reactions that lead to the formation of salts. These reactions are schematically illustrated in **Figure 1**–**Figure 3**, using the mono-, di- and trisodium salts as examples.

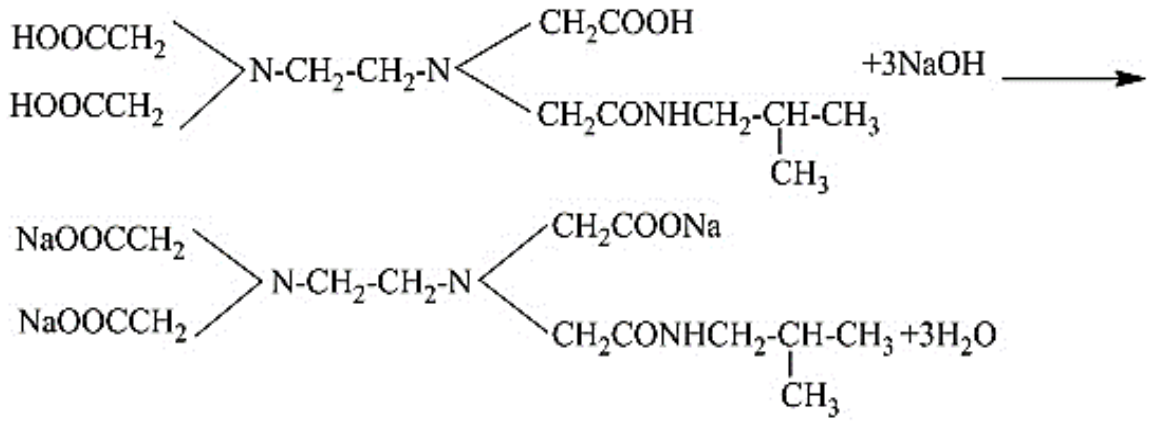


Figure 1. Preparation of the trisodium salt of monoisobutylamide of ethylenediaminetetraacetic acid

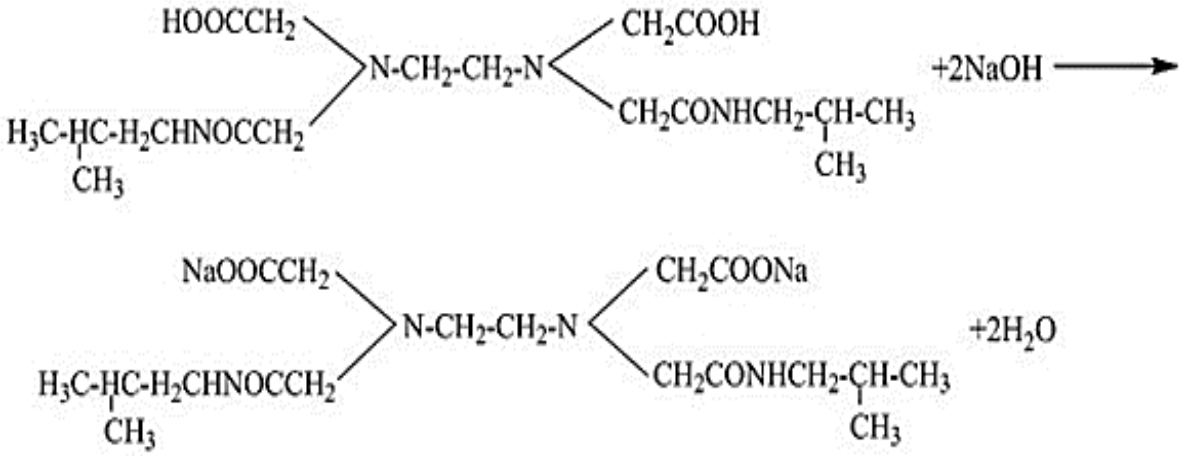


Figure 2. Preparation of the disodium salt of diisobutylamide of ethylenediaminetetraacetic acid

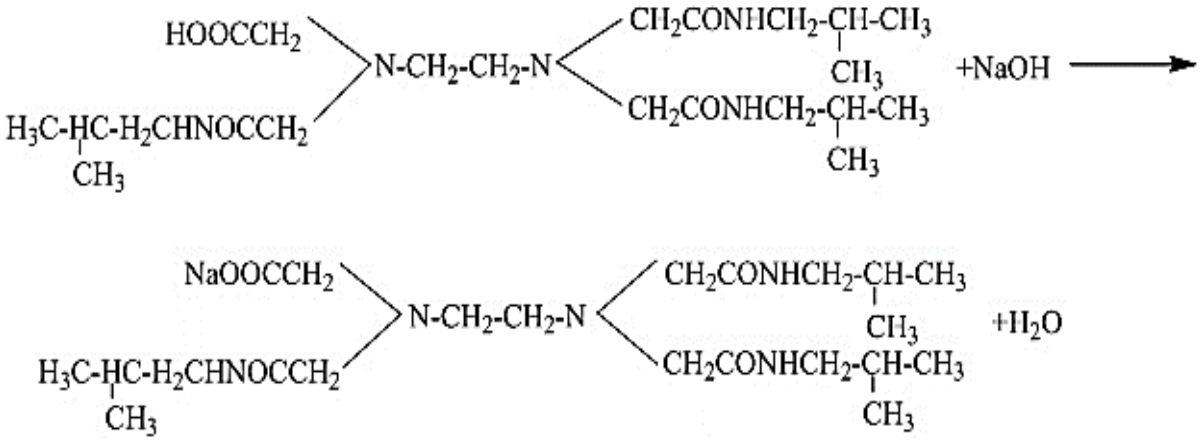


Figure 3. Preparation of the monosodium salt of triisobutylamideof ethylenediaminetetraacetic acid

Corrosion and Salt Precipitation Inhibition Tests and Measurements

Later, the inhibitory properties of the synthesised sodium and potassium salts of mono-, di-, and triisobutylamides of ethylenediaminetetraacetic acid against corrosion and salt deposition were studied using the methodology described in [50] with Steel-3 (low-carbon mild steel) metal plates sized 3 cm × 4 cm. To test the corrosion inhibitory properties, two 1000 mL beakers were filled with water from the experimental environment. The water used in the experiment was slightly alkaline (pH=8.47−8.51), with an electrical conductivity of 598−606 μS cm^{-1} and a dissolved oxygen concentration below 5 mg L^{-1}. It is similar to those in cooling tower systems. The mineral composition included 53−54 mg L^{-1} calcium, 19 mg L^{-1} magnesium, and 31−33 mg L^{-1} sodium ions. A predetermined amount of the examined salt was added to one of the beakers, and at least two plates were suspended in each beaker. The plates were polished beforehand, wiped with acetone, and dried using filter paper and cotton; their masses were measured with an analytical balance, and their surface areas were calculated. Both beakers were placed on magnetic stirrers equipped with heaters and stirred at 400 rpm. The experiments were conducted at 50 °C for 5 hours. The water temperature was controlled with a thermometer. The tests were carried out by adding salts to the medium at concentrations of 50, 100 and 150 mg L^{-1}. At the end of the experiment, the plates were removed from the water and immersed for one minute in a solution prepared by mixing hydrochloric acid and distilled water in a 1:1 volume ratio, with the addition of 4−6% formalin. The plates were then washed with distilled water, dried, wiped with acetone, and dried again.

After the experiment, the plates were weighed again on an electronic balance, and the corrosion rates were calculated for both the inhibited and uninhibited systems. The formula determined the mass loss of the metal plates:

$$\Delta m = m_2 - m_1 \tag{3}$$

where m_1 is the mass of the plate before the experiment and m_2 is the mass after the experiment (Δm was calculated as the average value for the plates). Then the corrosion rates without inhibitor V_0 and with inhibitor V_{inh} were calculated by the general equation:

$$V = \frac{\Delta m}{S \times t} \tag{4}$$

where V is the corrosion rate [mg cm^{-2} h^{-1}], Δm is the mass loss [mg], S is the surface area of the plate [cm^2], and t is the duration of the experiment [h]. Based on the corrosion rate values obtained before (V_o) and after (V_{inh}) the addition of the inhibitor, the effectiveness IE of the salts as corrosion inhibitors was calculated by the formula:

$$IE = \frac{V_0 - V_{inh}}{V_0} \times 100\% \tag{5}$$

To study the inhibitory properties against salt precipitation, the effectiveness was evaluated based on the difference in the rate of salt precipitation by measuring the concentration of Ca^{2+} ions before and after the experiment in media with and without inhibitors. At this stage, the Ca^{2+} ion concentration was determined by titration using Trilon B. Based on the amount of $CaCO_3$ formed, the rate of salt precipitation was calculated. The efficiency of the samples was determined using the same approach.

As stated in the methodology, the experiments were conducted in several repeated trials. It was ensured that the deviation between the measured values did not exceed 5% for corrosion

experiments and 8% for sedimentation experiments, and their average mathematical values were used in the calculations.

Computational Calculation Method

All Density Functional Theory (DFT) calculations were performed using the ORCA software package [51], [52]. Geometry optimisations were carried out at the B3LYP/6-31G(d) level of theory [53]–[55], using the same basis set for all atoms, including the metal ions. Frequency calculations were subsequently performed at the same level of theory on the optimised structures to confirm the nature of the stationary points and to obtain thermodynamic data. The Self-Consistent Field (SCF) convergence criterion was set to TightSCF with a maximum of 125 iterations, and all calculations were run in parallel using 44 processor cores.

RESULTS AND DISCUSSION

The physicochemical properties of the synthesised compounds and the structural confirmation by IR spectroscopy are presented. Their corrosion and salt-precipitation inhibition properties, as well as the adsorption mechanism and theoretical study, are also discussed.

Properties and Infrared Characterisation of the Synthesised Isobutylamide Derivatives of Ethylenediaminetetraacetic Acid

Aqueous solutions of the sodium and potassium salts of mono-, di-, and triisobutylamides of ethylenediaminetetraacetic acid were prepared at a concentration of 10%, and their main physicochemical properties, such as kinematic viscosity at 20°C ν [mm^2 s^{-1}], density ρ^{20} [g cm^{-3}], refractive index n_D^{20}, and freezing point T_{freezing} [°C], were determined. All data are presented in Table 1. The density values ranged from 1.0449 to 1.0484 g cm^{-3} for the sodium salts and from 1.0400 to 1.0463 g cm^{-3} for the potassium salts. The kinematic viscosities ranged from 1.3772 to 1.3830 mm^2 s^{-1} for the sodium salts and from 1.5454 to 1.5519 mm^2 s^{-1} for the potassium salts. The lowest freezing point among all the investigated solutions was −5 °C.

Table 1. Physicochemical characteristics of 10% aqueous solutions of the sodium and potassium salts of isobutylamides of ethylenediaminetetraacetic acid

Salts of isobutylamides of ethylenediaminetetraacetic acid	ρ^{20} [g cm^{-3}]	ν [mm^2 s^{-1}]	T_{freezing} [°C]	n_D^{20}
Trisodium salt	1.0484	1.3830	−5	1.3497
Disodium salt	1.0477	1.3775	−4	1.3473
Monosodium salt	1.0449	1.3772	−4	1.3408
Tripotassium salt	1.0463	1.5519	−5	1.3547
Dipotassium salt	1.0401	1.5454	−4	1.3567
Monopotassium salt	1.0400	1.5494	−4	1.3502

IR spectroscopy was used to confirm the structures of the synthesised compounds. The IR spectra were recorded using an ALPHA Fourier-transform infrared spectrometer manufactured by the German company Bruker. Figure 4 presents the IR spectra of the synthesised sodium and potassium salts of mono- and tri-isobutylamides of ethylenediaminetetraacetic acid. The assignments of the observed IR absorption bands are explained in Table 2.

As can be seen from the spectra and their interpretations in the table, absorption bands characteristic of amide and carboxylate groups are observed in the compounds. These bands correspond to the stretching vibrations of the amide C = O bonds at 1624 cm^{-1} (a), 1637 cm^{-1} (b), 1605 cm^{-1} (c), and 1634 cm^{-1} (d), as well as to the deformation vibrations of the amide N − H bonds at 1530 cm^{-1} (a), 1574 cm^{-1} (b), 1573 cm^{-1} (c), and 1577 cm^{-1} (d).

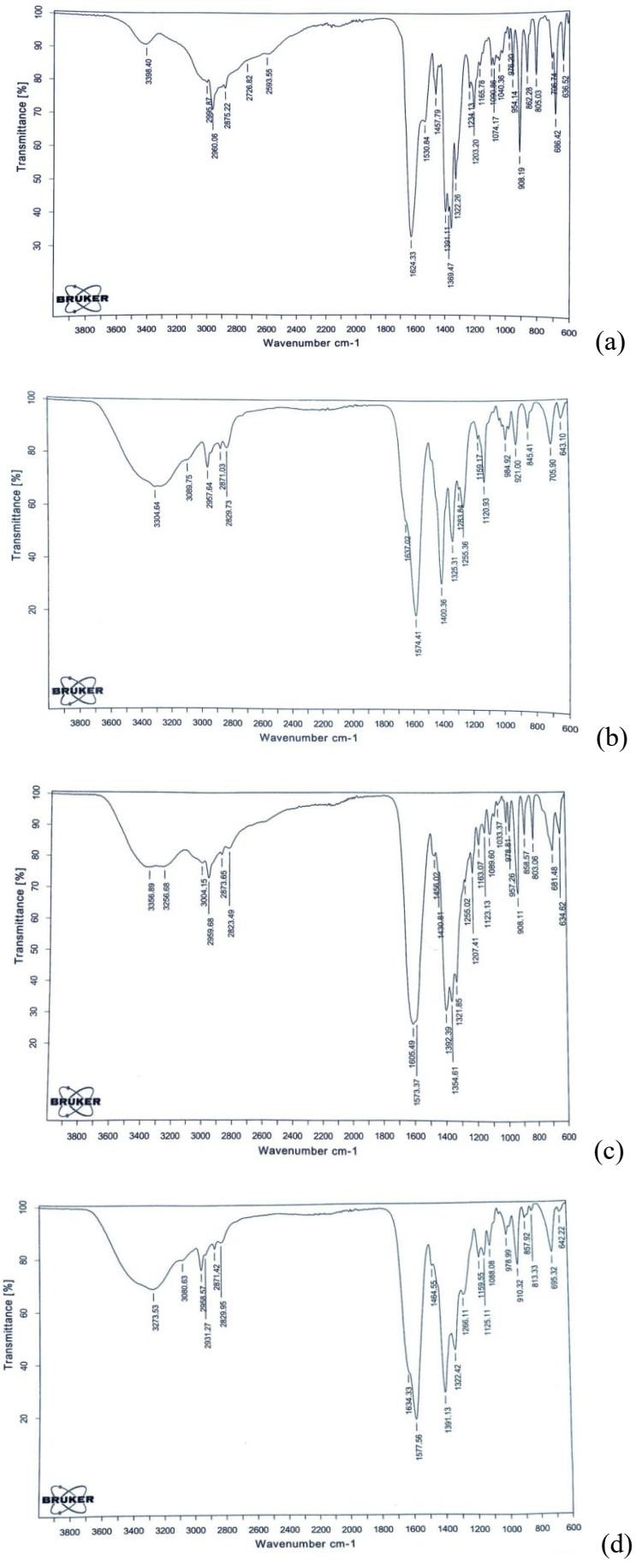


Figure 4. IR spectra of the trisodium (a), monosodium (b), tripotassium (c), and monopotassium (d) salts of isobutylamides of ethylenediaminetetraacetic acid

Table 2. Explanation of the observed spectra of the sodium and potassium salts of mono- andtriisobutylamides of ethylenediaminetetraacetic acid

Assignment	Wavenumber [cm^{-1}]			
	Trisodium salt	Monosodium salt	Tripotassium salt	Monopotassium salt
Deformation vibrations of the C – H and N – H bonds	636, 686, 706, 805, 862, 908, 954, 976	643, 705, 845, 921, 984	634, 681, 803, 858, 908, 957, 978	642, 695, 813, 857, 910, 978
Deformation and valence vibrations of the C – O and C – N bonds	1040, 1074, 1090, 1165, 1203, 1234	1120, 1159, 1255, 1283	1089, 1123, 1163, 1207, 1255	1088, 1125, 1159, 1266
Deformation and valence vibrations of the C – H bond	1322, 2875, 2960	1325, 2829, 2871, 2957	1321, 1354, 2823, 2873, 2959	1322, 2829, 2871, 2958
Carboxylate band	1391	1400	1392	1391
Amide band	1530, 1624	1574, 1637	1573, 1605	1577, 1634
Valence oscillation of the N – H bond	3398	3304	3256, 3356	3080, 3273

The absorption bands attributed to the symmetric stretching vibration of the carboxylate group were identified at 1391 cm^{-1} (a), 1400 cm^{-1} (b), 1392 cm^{-1} (c), and 1391 cm^{-1} (d). At the same time, it should be noted that the second absorption band of the carboxylate group, which is expected to appear in the 1550−1650 cm^{-1} region of the spectra, overlaps with the absorption bands of the amide groups. Additionally, the absence of a band near 1720 cm^{-1} indicates the complete conversion of carboxylic acid groups to the sodium salt form. The interpretation of the spectra confirms that amide groups were formed during the aminolysis process and that, upon treatment with an alkali to obtain their salts, the carboxyl groups were converted into carboxylate groups.

Inhibition efficiency, adsorption isotherm and mechanism of the synthesised compounds

The results of the experiments conducted to evaluate the effectiveness of the sodium and potassium salts of mono-, di-, and triisobutylamides of ethylenediaminetetraacetic acid against corrosion and salt deposition are given in **Table 3**.

As shown in **Table 3**, the corrosion protection efficiency of the sodium and potassium salts of mono-, di-, and triisobutylamides of ethylenediaminetetraacetic acid at concentrations of 50, 100 and 150 mg L^{-1} exceeded 70%. At a concentration of 50 mg L^{-1}, the highest efficiency (90%) was exhibited by the trisodium salt of monoisobutylamide of ethylenediaminetetracetic acid, whereas the lowest efficiency (70%) was observed for the monopotassium salt. Their inhibitory activity against salt precipitation exceeded 80%, with the trisodium salt again showing the highest efficiency (90%) and the monopotassium salt the lowest (80%) at the same concentration of 50 mg L^{-1}. Considering that the inhibition efficiencies of the sodium and potassium salts of mono-, di-, and triisobutylamides of ethylenediaminetetraacetic acid at concentrations of 50, 100, and 150 mg L^{-1} exceed 70% for corrosion and 80% for salt deposition, it can be concluded that these compounds exhibit quite high effectiveness.

Table 3. Corrosion and salt deposition inhibitory properties of the sodium and potassium salts ofmono-, di-, and triisobutylamides of ethylenediaminetetraacetic acid

Salt	Salt concentration, [mg L^{-1}]	Effectiveness [%]	
		Anti-corrosion	Against salt deposition
Trisodium salt of monoisobutylamide of EDTA	50	90	90
	100	96	96
	150	99	98
Disodium salt of diisobutylamide of EDTA	50	88	85
	100	95	92
	150	98	94
Monosodium salt of triisobutylamide of EDTA	50	87	82
	100	94	89
	150	97	93
Tripotassium salt of monoisobutylamide of EDTA	50	74	84
	100	79	88
	150	83	90
Dipotassium salt of diisobutylamide of EDTA	50	72	82
	100	78	85
	150	82	89
Monopotassium salt of triisobutylamide of EDTA	50	70	80
	100	73	81
	150	80	88

The highest result was obtained with the trisodium salt of monoisobutylamide of ethylenediaminetetraacetic acid at a concentration of 50 mg L^{-1}; at concentrations of 100 and 150 mg L^{-1}, it demonstrated 96% and 99% effectiveness against corrosion, and 96% and 98% effectiveness against salt precipitation, respectively. It should be noted that when sodium and potassium salts of mono-, di-, and triisobutylamides of ethylenediaminetetraacetic acid were used at concentrations of 100 and 150 mg L^{-1}, their performance in both corrosion inhibition and anti-scaling activity was higher. As shown in the graphical representations in **Figure 5**, effectiveness increased with increasing concentration.

It was determined that, overall, among the synthesised salts, the isobutylamides of ethylenediaminetetraacetic acid in the form of trisodium and tripotassium salts exhibit the highest effectiveness against corrosion and salt precipitation. Since the number of anionic groups adsorbed on the surface is higher in the trisodium and tripotassium salts, they provide greater surface coverage and stronger adsorption, forming a more effective coating compared with mono- or disubstituted salts. This tendency, in turn, provides better protection against corrosion and reduces salt precipitation **[56]**, **[57]**. At the same time, the results indicate that a higher number of anionic groups in the molecule enhances salt precipitation inhibition by forming coordination complexes with the cations responsible for scale deposition, thereby reducing their free concentration in solution and preventing their precipitation as insoluble salts **[58]**, **[59]**. The order of activity as corrosion and salt precipitation inhibitor for both sodium and potassium salts was found to be mono-<di-<tri-.

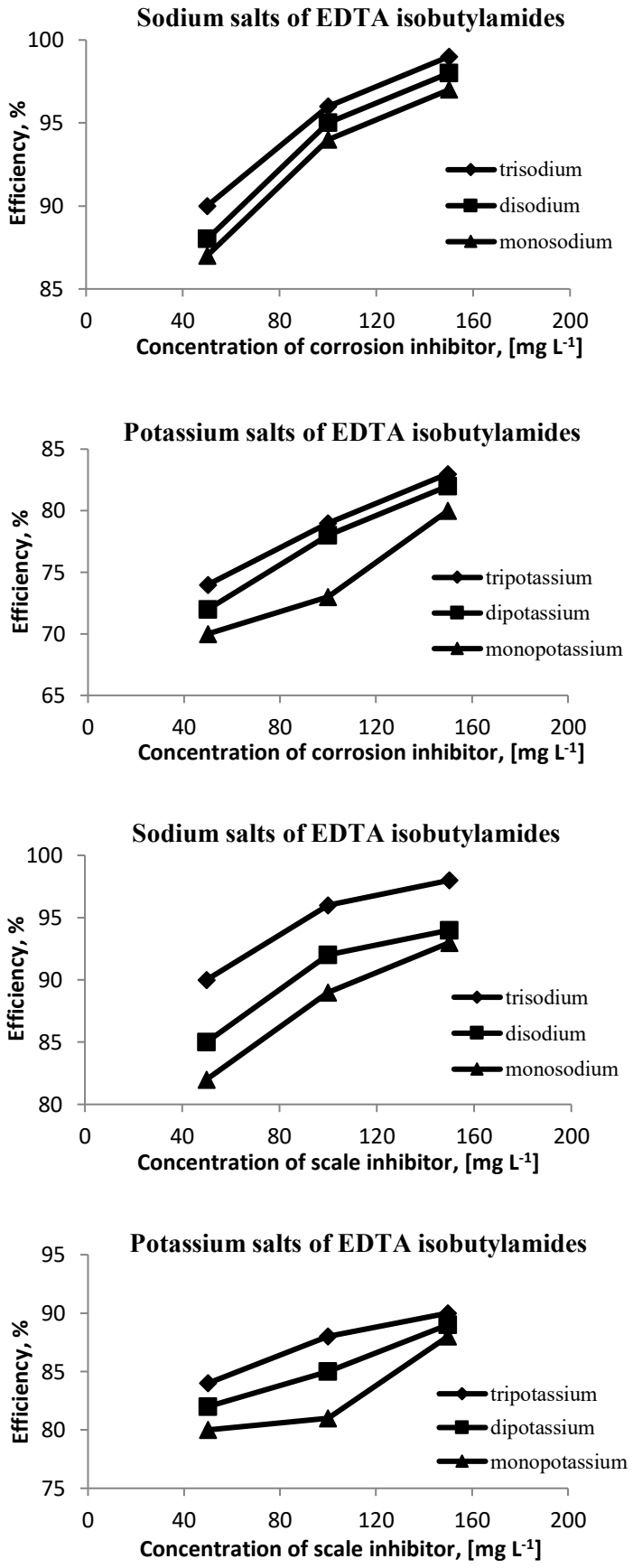


Figure 5. Concentration dependence of the corrosion and salt precipitation inhibitory properties of the sodium and potassium salts of mono-, di-, and triisobutylamides of ethylenediaminetetraacetic acid

The results also showed that mono-, di- and trisodium salts of isobutylamides of ethylenediaminetetraacetic acid are more effective as corrosion inhibitors than the corresponding potassium salts. The higher effectiveness of sodium salts compared with the corresponding potassium salts can be attributed to differences in ion size, hydration, and adsorption behaviour. Sodium ions, being smaller and more strongly hydrated than potassium ions, exhibit stronger solvation in aqueous solutions, thereby promoting better dissociation of sodium salts and facilitating the release of free anions [60], [61]. Thereby, a more uniform distribution and stronger adsorption of the inhibitor anions on the metal surface are achieved.

As is well known, the inhibition efficiency depends directly on the surface area covered by adsorbed inhibitor molecules. The degree of surface coverage θ can be calculated using corrosion rate values obtained from weight loss measurements at 323 K, according to the following equation:

$$\theta = 1 - \frac{V_{inh}}{V_0} \tag{6}$$

where V_0 and V_{inh} represent the corrosion rates [mg cm^{-2} h^{-1}] in the absence and presence of the inhibitor, respectively.

The obtained data are summarised in Table 4. The results indicate that increasing the inhibitor concentration increases surface coverage and decreases the corrosion rate. The high surface coverage value, close to unity, indicates nearly complete coverage of the investigated metal surface by adsorbed molecules. Thus, the surface is efficiently isolated from the corrosive medium. In the absence of the inhibitor, the corrosion rate was found to be 0.59 mg cm^{-2} h^{-1}.

Table 4. Corrosion rate and surface coverage data obtained from weight loss measurements for Steel-3 metal plates in the absence and presence of the sodium and potassium salts of mono-, di-, and triisobutylamides of ethylenediaminetetraacetic acid

Salt	Salt concentration, [mg L^{-1}]	Corrosion rate, [mg cm^{-2} h^{-1}]	Surface coverage
Trisodium salt of monoisobutylamide of EDTA	50	0.0573	0.90
	100	0.0231	0.96
	150	0.0118	0.98
Disodium salt of diisobutylamide of EDTA	50	0.0884	0.85
	100	0.0468	0.92
	150	0.0353	0.94
Monosodium salt of triisobutylamide of EDTA	50	0.1056	0.82
	100	0.0642	0.89
	150	0.0411	0.93
Tripotassium salt of monoisobutylamide of EDTA	50	0.0941	0.84
	100	0.0703	0.88
	150	0.0575	0.90
Dipotassium salt of diisobutylamide of EDTA	50	0.1055	0.82
	100	0.0883	0.85
	150	0.0648	0.89
Monopotassium salt of triisobutylamide of EDTA	50	0.118	0.80
	100	0.1118	0.81
	150	0.0706	0.88

Fundamental insights into the interaction between inhibitor molecules and metal surfaces can be obtained by analysing adsorption isotherms. To establish the adsorption isotherm, the degree of surface coverage as a function of inhibitor concentration must be determined. The applicability of the Langmuir adsorption isotherm was evaluated by fitting the experimental data on the correlation between the degree of surface coverage and the inhibitor concentration in the corrosive medium. The Langmuir isotherm is expressed as follows:

$$\frac{C_{inh}}{\theta} = C_{inh} + \frac{1}{K_{ads}} \tag{7}$$

where C_{inh} is the molar concentration of the inhibitor, and K_{ads} is the equilibrium constant of the inhibitor adsorption process.

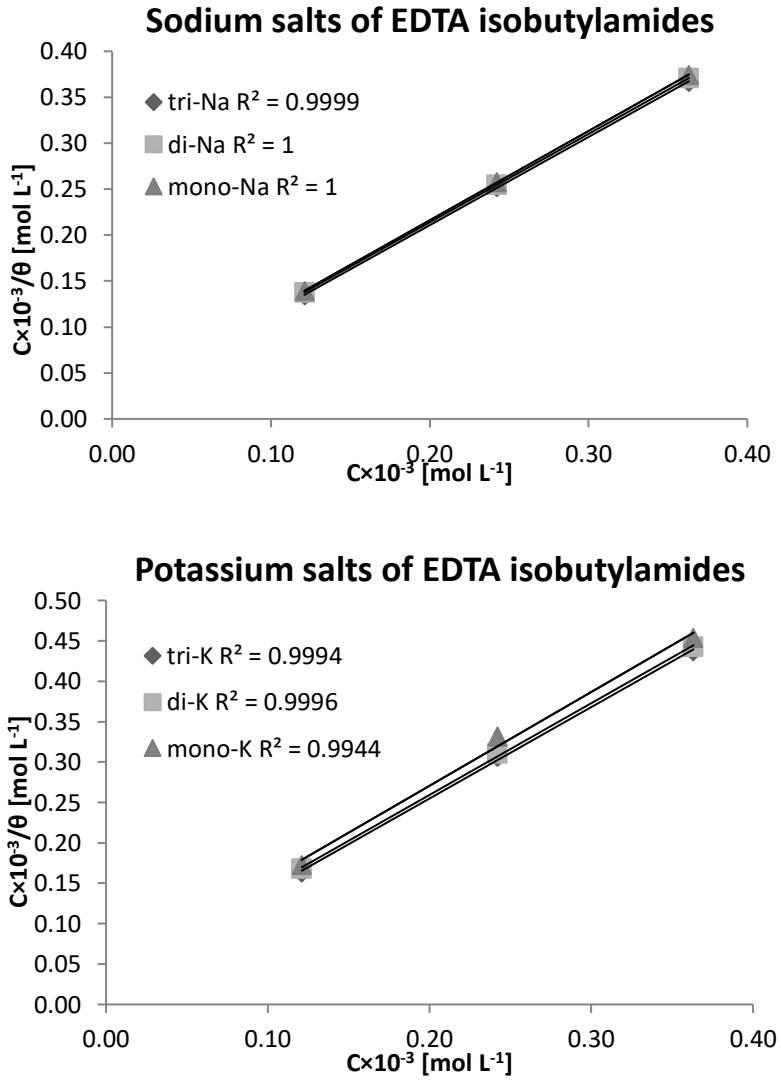


Figure 6. Langmuir adsorption isotherm plots for the sodium and potassium salts of mono-, di-, and triisobutylamides of ethylenediaminetetraacetic acid

When a graph of C_{inh}/θ versus C_{inh} was plotted, a straight line with linear correlation coefficients R^2 close to unity was obtained, as shown in **Figure 6**. This indicates that the adsorption of the investigated inhibitors on the metal surface at 323 K follows the Langmuir adsorption isotherm model. The corresponding linear regression coefficients are also presented in **Figure 6**.

The reciprocal intercept values of the Langmuir plots are equal to the adsorption equilibrium constant, which represents the degree of adsorption and is related to the standard free energy of adsorption through the following expression:

$$K_{ads} = \frac{1}{55.5}\, exp(-\frac{\Delta G^0_{ads}}{RT}) \quad (8)$$

where ΔG^o_{ads} is the change in Gibbs free energy, K_{ads} is the adsorption equilibrium constant, R is the universal gas constant 8.314 J K^{-1} mol^{-1}, T is the absolute temperature, and 55.5 mol L^{-1} is the concentration of water.

The values of K_{ads} were used to calculate the standard free energy of adsorption, which characterises the interaction of inhibitor molecules with the metal surface, and the results are presented in **Table 5**. The relatively high values of the adsorption equilibrium constant reflect the strong adsorption ability of these salts on the metal surface.

Table 5. Thermodynamic parameters for the adsorption of the sodium and potassium salts of mono-, di-, and triisobutylamides of ethylenediaminetetraacetic acid

Salts of isobutylamides of ethylenediaminetetraacetic acid	$K_{ads} \times 10^4$ [M^{-1}]	ΔG^o_{ads} [kJ mol^{-1}]
Trisodium salt	5.291	−39.99
Disodium salt	4.695	−39.67
Monosodium salt	4.587	−39.61
Tripotassium salt	3.497	−38.88
Dipotassium salt	3.086	−38.55
Monopotassium salt	2.597	−38.08

The mechanism of corrosion inhibition may be explained based on the adsorption behaviour of the compounds. The adsorption of corrosion inhibitors on metal surfaces involves two principal types of interactions responsible for the binding process. The first, physical adsorption (physisorption), is characterised by weak, non-directional interactions arising from electrostatic attraction between charged inhibitor species or dipolar molecules and the electrically charged metal surface. The second, chemical adsorption (chemisorption), occurs through stronger, directional interactions, in which charge sharing or transfer takes place between inhibitor molecules and metal surface atoms, leading to the formation of coordinate bonds.

Based on the obtained values of ΔG^o_{ads}, it is possible to predict the adsorption mechanism of inhibitor molecules on the metal surface. In comparison with physisorption, chemisorption is associated with higher adsorption free energy and activation energy and is therefore generally considered irreversible. Typically, ΔG^o_{ads} values around −20 kJ mol^{-1} or less negative are characteristic of physisorption, whereas values around −40 kJ mol^{-1} or more negative indicate chemisorption.

The high negative values of ΔG^o_{ads} (**Table 5**), obtained for the synthesised molecules, indicate the spontaneous nature of the adsorption process and the stability of the adsorbed layer on the metal surface, suggesting that adsorption occurs via a chemisorption mechanism. Chemisorption occurs when inhibitor molecules adsorb onto the metal surface via their functional groups, involving interactions between the d-orbitals of iron atoms and the lone pairs on the sp^2-hybridised nitrogen and oxygen atoms of the inhibitor.

This is because the interaction energy between the inhibitor molecules and the metal surface is higher than that between water molecules and the metal surface, leading to the displacement of water molecules from the surface. Adsorption of inhibitor molecules from an aqueous solution can be regarded as a quasi-substitution process between inhibitor species in the solution and water molecules adsorbed on the metal surface. Consequently, the protective

action of the studied inhibitors during metal corrosion is based on their adsorption ability, whereby the resulting adsorbed film isolates the metal surface from the corrosive medium. Overall, the inhibition efficiency of these compounds is influenced by several factors, including the number and charge density of adsorption-active centres, molecular size, and the nature of the interaction between inhibitor molecules and the metal surface.

Theoretical Study

In recent years, atomistic simulations have emerged as a unique and powerful computational tool for advancing corrosion inhibition research [62]. Density Functional Theory is now widely used to elucidate the correlation between molecular structure and inhibition performance, providing a theoretical foundation for experimental observations in aggressive environments such as desalination plants [59], [63]. By calculating critical quantum-chemical parameters, including frontier molecular orbital distributions and the fraction of electron transfer, researchers can elucidate the specific interaction mechanisms of inhibitors at the metal-electrolyte interface [64], [65]. This computational approach is particularly vital for evaluating multifunctional reagents such as EDTA derivatives, as it confirms the role of nucleophilic centres in achieving high protection efficiencies [66].

To provide a theoretical foundation for the experimental observations and to elucidate the structure-activity relationship of the synthesised compounds, DFT calculations were conducted. The primary objective was to investigate the electronic properties and optimised molecular geometries of the inhibitors to understand how their spatial arrangement and functional group distribution influence the interaction with the metal surface. The optimised geometries of the trisodium, monosodium, and tripotassium salts are illustrated in Figure 7.

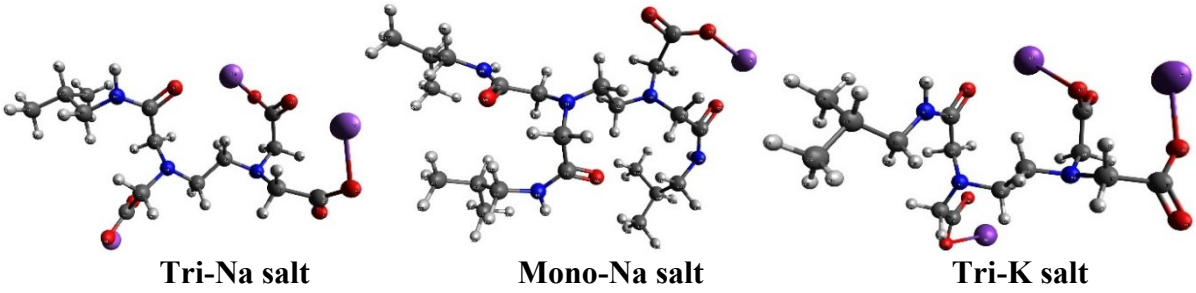


Figure 7. Optimised molecular structures of the trisodium salt, monosodium salt, and tripotassium salt of isobutylamides of ethylenediaminetetraacetic acid

The optimised structures reveal that the carboxylate groups ($-COO^-$) and the amide linkages ($-CONH-$) act as the primary nucleophilic centres for coordination with the Steel-3 surface. The $C-O$ bond lengths in the carboxylate groups (ranging from 0.123 to 0.128 nm) and the $C=O$ bond lengths in the amide groups confirm that these sites are electron-rich, facilitating the formation of protective layers via chemisorption, as established by the Langmuir isotherm. Consistent with findings in the existing literature on EDTA analogues [47], the "tri-" substituted salts (trisodium and tripotassium) exhibit a more extended and planar spatial configuration due to the presence of three anionic carboxylate groups. This configuration allows the molecule to occupy a larger surface area on the metal substrate, leading to the higher surface coverage θ observed in the corrosion experiments. In contrast, the monosodium salt adopts a more "curled" geometry, which effectively reduces its adsorption footprint and explains its lower efficiency (70–80%) compared to the trisodium salt (90–99%). The calculated bond lengths between the alkali metal ions and the oxygen atoms (approximately 0.210–0.217 nm for $Na-O$ and 0.240–0.265 nm for $K-O$) correlate with the experimental finding that sodium salts outperform potassium salts. The shorter, more specific coordination in the sodium derivatives, combined

with their smaller ionic radius and stronger hydration, facilitates more uniform dissociation and distribution of the inhibitor anions at the metal-water interface.

Furthermore, to evaluate the electronic interactions and identify the specific sites responsible for electron exchange with the metal surface, the frontier molecular orbital distributions were analysed (**Figure 8**).

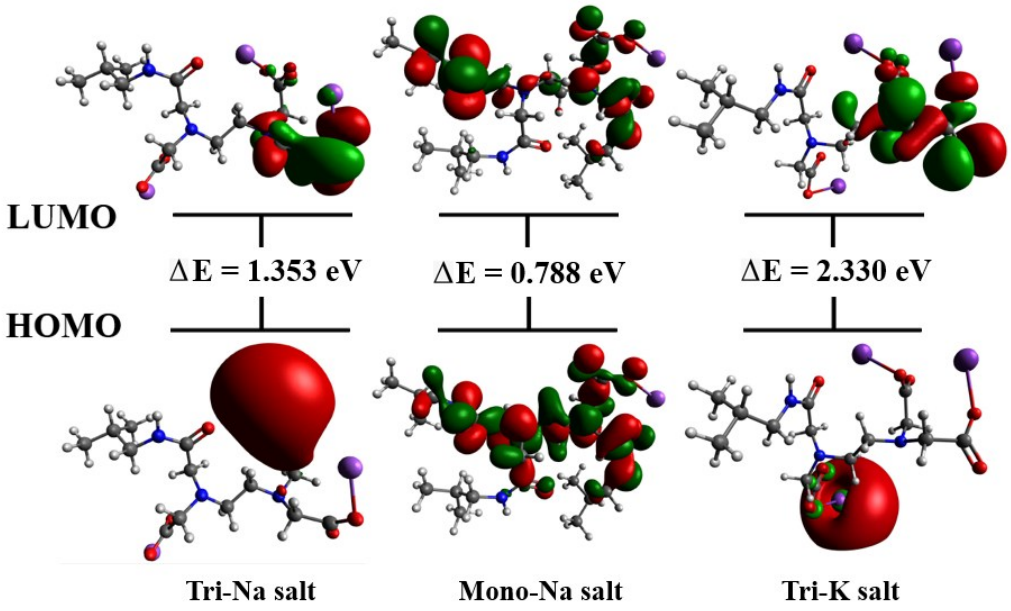


Figure 8. Spatial distribution of HOMO and LUMO density for the optimised structures of thetrisodium salt, monosodium salt, and tripotassium salt of isobutylamides of ethylenediaminetetraacetic acid

As shown in **Figure 8**, the highest occupied molecular orbital (HOMO) density is primarily localised over the carboxylate groups ($-COO^-$) and the nitrogen atoms of the ethylenediamine core. Such localisation confirms that these regions are the primary nucleophilic centres donating electrons to the vacant d-orbitals of the iron atoms on the Steel-3 surface. The concentration of HOMO density on the three carboxylate groups in the trisodium and tripotassium salts supports their superior performance, as they offer more "anchoring points" for chemical interactions than the monosodium salt. The lowest unoccupied molecular orbital (LUMO) density is largely distributed across the amide linkages ($-CONH-$) and the carbonyl oxygens. This distribution suggests that these groups can accept back-donated electrons from the metal surface, strengthening the adsorption bond through a synergic mechanism. The broad spatial distribution of both HOMO and LUMO throughout the molecular framework in the trisodium salt indicates a high chemical reactivity and a strong tendency to form a stable, flat-oriented protective film. This molecular "footprint" aligns with the experimental observation that trisodium achieves 99% protection efficiency, as the orbital overlap with the metal surface is maximised in this configuration. The localisation of electron density on the carboxylate oxygens also explains the high scale-prevention efficiency (90–98%). These electron-rich regions act as effective chelating sites for Ca^{2+} ions, preventing their precipitation as scale.

In addition to the visual analysis of orbital distributions, several global quantum-chemical parameters were calculated to quantitatively assess the reactivity and stability of the inhibitors. These parameters, including ionisation potential, electron affinity, electronegativity, chemical hardness, and the fraction of electrons transferred, were determined based on the frontier molecular orbital energies (E_{HOMO} and E_{LUMO}) in accordance with established literature methodologies for corrosion inhibition studies **[67]**–**[69]**.

The calculated quantum chemical parameters presented in **Table 6** provide a robust theoretical framework for understanding the high inhibition efficiencies observed in the experimental trials. According to the Frontier Molecular Orbital theory, the interaction between the inhibitor and the metal surface is governed by the HOMO and LUMO energy levels. To calculate the fraction of electrons transferred ΔN, the theoretical values for the absolute electronegativity and chemical hardness of bulk iron were utilised. Following the established literature on corrosion studies of steel, the electronegativity of iron was taken as $\chi\mathrm{Fe} = 7.0$ eV and the chemical hardness as $\eta\mathrm{Fe} = 0$ eV, assuming that the metal surface acts as a soft soft-acid sea of electrons [70]. These reference values enable a direct quantitative assessment of the electron-donating capability of the synthesised inhibitors toward the Steel-3 substrate.

Table 6. Calculated quantum chemical parameters for the optimised structures of the trisodium salt, monosodium salt, and tripotassium salt of isobutylamides of ethylenediaminetetraacetic acid

Parameter	Salts of isobutylamides of ethylenediaminetetraacetic acid		
	trisodium salt	monosodium salt	tripotassium salt
E_{HOMO} [eV]	−3.817	−5.140	−3.612
E_{LUMO} [eV]	−2.464	−4.352	−1.282
Energy Gap E_{gap} [eV]	1.353	0.788	2.330
Ionisation Potential I [eV]	3.817	5.140	3.612
Electron Affinity A [eV]	2.464	4.352	1.282
Electronegativity χ [eV]	3.141	4.746	2.447
Chemical Potential μ [eV]	−3.141	−4.746	−2.447
Chemical Hardness η [eV]	0.677	0.394	1.165
Chemical Softness σ [eV^{-1}]	0.739	1.269	0.429
Electrophilicity Index ω [eV]	7.287	28.586	2.570
Fraction of electrons transferred ΔN	2.850	2.860	1.954

The fraction of electrons transferred is a critical indicator of the strength of chemical adsorption. The calculated ΔN values for all studied inhibitors are positive, confirming that the mechanism of inhibition involves electron donation from the inhibitor's active centres (carboxylate and amide groups) to the vacant d-orbitals of the iron atoms. Notably, the ΔN values for the sodium salts (trisodium: 2.850; monosodium: 2.860) are significantly higher than that of the potassium salt (tripotassium: 1.954). This theoretical finding perfectly supports the experimental evidence that sodium-based derivatives provide superior corrosion protection. According to the Hard-Soft Acid-Base principle, "soft" molecules (lower η) are more reactive and tend to form stronger coordinate bonds with metal surfaces. The trisodium salt exhibits a lower chemical hardness (0.677 eV) compared to the tripotassium salt (1.165 eV), indicating that the sodium derivative is more polarizable and can more effectively interact with the Steel-3 surface to form a stable protective film.

The energy gap ($E_{LUMO} - E_{HOMO}$) is an indicator of the kinetic stability and reactivity of the molecule. The relatively low energy gaps for the trisodium and monosodium salts suggest higher reactivity at the metal-electrolyte interface, which aligns with the rapid formation of the protective layer observed in the weight-loss and scale-prevention tests. The absolute electronegativity values reflect the tendency of the molecules to attract electrons. The balance between χ and η in the trisodium salt optimises its role as an electron donor, consistent with the 99% inhibition efficiency and 98% scale prevention measured at 150 mg L^{-1} [70]–[72].

By aligning these quantum-chemical parameters with the experimental data, it is evident that the trisodium salt of EDTA isobutylamide possesses the most favourable electronic profile for multifunctional protection. The higher electron-transfer capability and lower molecular hardness of the sodium derivatives explain their dominant performance over the potassium-based analogues in 50 °C aqueous environments.

CONCLUSIONS

The sodium and potassium salts of isobutylamides of ethylenediaminetetraacetic acid were synthesised, their structures were confirmed by IR spectroscopy, and their 10% solutions were prepared to determine the main physicochemical properties. The synthesised salts were tested as corrosion and scale formation inhibitors at 50 °C, and it was determined that the sodium salts are more effective than the potassium salts, with their activity ranking in the order of mono-<di-<tri-.

The highest efficiency as a corrosion and salt precipitation inhibitor at a concentration of 50 mg L^{-1} was achieved with the trisodium salt of monoisobutylamide of ethylenediaminetetraacetic acid. At this concentration, it protected the Steel-3 metal plate from corrosion by 90%, and its effectiveness against salt deposition was 90% as well. The inhibitory properties against corrosion and salt deposition increased when the salt was added to the medium at concentrations of 100 and 150 mg L^{-1}. At the same time, it was determined that the effectiveness of all synthesised salts as corrosion and scale inhibitors was directly proportional to their concentration.

The adsorption behaviour of the studied compounds on the steel surface obeyed the Langmuir adsorption isotherm, while the obtained standard free energy of adsorption values confirmed that the mechanism is chemisorption.

Quantum-chemical calculations revealed that among the synthesised compounds, the sodium salts – particularly the trisodium salt – exhibited higher electron-transfer capabilities (ΔN = 2.850) compared to their potassium analogues. DFT analysis confirmed that the three anionic carboxylate centres in the trisodium salt facilitated a broader spatial configuration and maximised orbital overlap with the metal surface, providing a theoretical basis for its peak protection efficiency of 99%. These theoretical descriptors perfectly align with the experimentally established activity order of mono-<di-<tri-, validating the role of multicenter coordination in enhancing multifunctional inhibition performance.

Nomenclature

Symbols

A	electron affinity	[eV]
C_{inh}	molar concentration of the inhibitor	[mol L^{-1}]
E_{gap}	energy gap	[eV]
E_{HOMO}	energy of the highest occupied molecular orbital	[eV]
E_{LUMO}	energy of the lowest unoccupied molecular orbital	[eV]
ΔG^0_{ads}	standard free energy of adsorption	[kJ mol^{-1}]
I	ionization potential	[eV]
IE	effectiveness	[%]
K_{ads}	equilibrium constant of the inhibitor adsorption	
m_1	mass of the plate before experiment	[mg]
m_2	mass of the plate after experiment	[mg]
Δm	mass loss	[mg]
ΔN	fraction of electrons transferred	
R	universal gas constant	[J K^{-1} mol^{-1}]
R^2	correlation coefficient	-
S	surface area	[cm^2]
t	duration	[h]
T	absolute temperature	[K]
$T_{freezing}$	freezing point	[°C]
V	corrosion rate	[g m^{-2} h^{-1}]
V_{inh}	corrosion rate in presence of inhibitor	[g m^{-2} h^{-1}]
V_0	corrosion rate without inhibitor	[g m^{-2} h^{-1}]

Greek letters

η	chemical hardness	[eV]
θ	degree of surface coverage	-
μ	chemical potential	[eV]
v	kinematic viscosity	[$mm^2\ s^{-1}$]
ρ	density	[$g\ cm^{-3}$]
σ	chemical softness	[eV^{-1}]
χ	electronegativity	[eV]
ω	electrophilicity index	[eV]

Abbreviations

DFT	Density Functional Theory
EDTA	Ethylenediaminetetraacetic Acid
HOMO	Highest Occupied Molecular Orbital
LUMO	Lowest Unoccupied Molecular Orbital
ORCA	Quantum chemistry program
SCF	Self-Consistent Field

REFERENCES

1. K. D. Demadis, E. Mavredaki, A. Stathoulopoulou, E. Neofotistou, and C. Mantzaridis, Industrial water systems: problems, challenges and solutions for the process industries, *Desalination*, Vol. 213, No. 1–3, pp 38–46, Jul. 2007, https://doi.org/10.1016/j.desal.2006.01.042.
2. J. Li, M. Tang, Z. Ye, L. Chen, and Y. Zhou, Scale formation and control in oil and gas fields: A review, *Journal of Dispersion Science and Technology*, Vol. 38, No. 5, pp 661–670, May 2017, https://doi.org/10.1080/01932691.2016.1185953.
3. S. E. Coetser and T. E. Cloete, Biofouling and Biocorrosion in Industrial Water Systems, *Critical Reviews in Microbiology*, Vol. 31, No. 4, pp 213–232, Jan. 2005, https://doi.org/10.1080/10408410500304074.
4. O. S. I. Fayomi, I. G. Akande, and S. Odigie, Economic Impact of Corrosion in Oil Sectors and Prevention: An Overview, *J. Phys.: Conf. Ser.*, Vol. 1378, No. 2, 022037, Dec. 2019, https://doi.org/10.1088/1742-6596/1378/2/022037.
5. M. M. Vazirian, T. V. J. Charpentier, M. De Oliveira Penna, and A. Neville, Surface inorganic scale formation in oil and gas industry: As adhesion and deposition processes, *Journal of Petroleum Science and Engineering*, Vol. 137, pp 22–32, Jan. 2016, https://doi.org/10.1016/j.petrol.2015.11.005.
6. G. R. Puchina, V. V. Ragulin, A. G. Telin, *et al.*, Modern practice of salt deposition preventing and removing, *NGD*, Vol. 18, No. 2, pp 72–80, Jun. 2020, https://doi.org/10.17122/ngdelo-2020-2-72-80.
7. Abbasov V.M. , Alieva, L. I., Efendieva, L. M., *et al.*, *Reagents and Products for the Oil, Gas, Oil Refining and Petrochemical Industries*. Baku: Elm, 2017.
8. M. S. Kamal, I. Hussein, M. Mahmoud, A. S. Sultan, and M. A. S. Saad, Oilfield scale formation and chemical removal: A review, *Journal of Petroleum Science and Engineering*, Vol. 171, pp 127–139, Dec. 2018, https://doi.org/10.1016/j.petrol.2018.07.037.
9. R. D. Vidic, W. Liu, H. Li, and C. He, Water Treatment Chemicals: Types, solution chemistry, and applications, in *Mineral Scales and Deposits*, Elsevier, 2015, pp 169–191. https://doi.org/10.1016/B978-0-444-63228-9.00008-5.

10. V. M. Abbasov, Hany M. Abd El-Lateef, L. I. Aliyeva, *et al.*, Applicability of novel anionic surfactant as a corrosion inhibitor of mild steel and for removing thin petroleum films from water surface, *American Journal of Materials Science and Engineering*, Vol. 1, No. 2, pp 18–23, 2013, https://doi.org/10.12691/ajmse-1-2-1, https://pubs.sciepub.com/ajmse/1/2/1/index.html, [Accessed: Aug. 25, 2026].
11. S. Zhang *et al.*, Enhanced scale inhibition against $Ca_3(PO_4)_2$ and Fe_2O_3 in water using multi-functional fluorescently-tagged antibacterial scale inhibitors, *Environ. Sci.: Water Res. Technol.*, Vol. 6, No. 4, pp 951–962, 2020, https://doi.org/10.1039/C9EW01036J.
12. I. T. Ismayilov, Synthesis and properties of the multifunctional anticorrosive reagents on the basis of sunflower oil and ethanolamines, *Processes of Petrochemistry and Oil Refining*, Vol. 17, No. 4, pp 331–345, 2016.
13. Yu. I. Kuznetsov, Triazoles as a class of multifunctional corrosion inhibitors. A review. Part I. 1,2,3-Benzotriazole and its derivatives. Copper, zinc and their alloys, *Int. J. Corros. Scale Inhib.*, Vol. 7, No. 3, pp 271–307, Oct. 2018, https://doi.org/10.17675/2305-6894-2018-7-3-1.
14. Y. Hu, C. Chen, and S. Liu, State of art bio-materials as scale inhibitors in recirculating cooling water system: a review article, *Water Science and Technology*, Vol. 85, No. 5, pp 1500–1521, Mar. 2022, https://doi.org/10.2166/wst.2022.027.
15. N. D. Nabiyeva, *et al.*, Study of inhibitory-bactericidal properties of the byproduct of white oil production against deemulsifier and corrosion, *Processes of Petrochemistry and Oil Refining*, Vol. 22, No. 4, pp 546–551, 2021, https://ppor.az/index.php/ppor/article/view/277.
16. I. T. Ismayilov, *et al.*, Enhanced corrosion inhibition of mild steel in CO_2-saturated solutions containing some novel green surfactants based on cottonseed oil, *Int. J. Corros. Scale Inhib.*, Vol. 4, No. 1, pp 057–074, 2015, https://doi.org/10.17675/2305-6894-2015-4-1-057-074.
17. V. M. Abbasov, I. T. Ismayilov, H. M. Abd El-Lateef, and S. F. Akhmadbeyova, Anti-corrosive activities of some novel surfactants based on vegetable oils, *European Chemical Bulletin*, Vol. 3, No. 5, pp 437–440, 2014.
18. D.-J. Choi, S.-J. You, and J.-G. Kim, Development of an environmentally safe corrosion, scale, and microorganism inhibitor for open recirculating cooling systems, *Materials Science and Engineering: A*, Vol. 335, No. 1–2, pp 228–235, Sep. 2002, https://doi.org/10.1016/S0921-5093(01)01928-1.
19. M. A. Jafar Mazumder, A Review of Green Scale Inhibitors: Process, Types, Mechanism and Properties, *Coatings*, Vol. 10, No. 10, 928, Sep. 2020, https://doi.org/10.3390/coatings10100928.
20. X. Wang, J. Yang, X. Chen, C. Liu, and J. Zhao, Synergistic inhibition properties and microstructures of self-assembled imidazoline and phosphate ester mixture for carbon steel corrosion in the CO_2 brine solution, *Journal of Molecular Liquids*, Vol. 357, 119140, Jul. 2022, https://doi.org/10.1016/j.molliq.2022.119140.
21. S. Bahrami, A. E. S. Van Driessche, M. F. Mady, and R. Panahi, A Synergistic Approach to Develop Sustainable Scale Inhibitors Combining Amino Acids and Polyphosphates, *Water Air Soil Pollut*, Vol. 235, No. 7, 456, Jul. 2024, https://doi.org/10.1007/s11270-024-07289-w.
22. F. Liu *et al.*, Optimizations of inhibitors compounding and applied conditions in simulated circulating cooling water system, *Desalination*, Vol. 313, pp 18–27, Mar. 2013, https://doi.org/10.1016/j.desal.2012.11.028.
23. R. Ketrane, B. Saidani, O. Gil, L. Leleyter, and F. Baraud, Efficiency of five scale inhibitors on calcium carbonate precipitation from hard water: Effect of temperature and concentration, *Desalination*, Vol. 249, No. 3, pp 1397–1404, Dec. 2009, https://doi.org/10.1016/j.desal.2009.06.013.

24. Z. Amjad and K. Demadis, *Water-Formed Deposits: Fundamentals and Mitigation Strategies*. Amsterdam: Elsevier, 2022.
25. N.A. Karpunin, A. A. Ryazanov, L. N. Khromyh and N. A. Shukin, Modern experience handling bottomhole formation zone of terrigenous deposit by acid compositions, *The Eurasian Scientific Journal*, Vol. 4, No. 10, 42NZVN418, 2018, https://esj.today/PDF/42NZVN418.pdf, [Accessed: Aug. 25, 2026].
26. P. Zhang, D. Shen, G. Ruan, A. T. Kan, and M. B. Tomson, Phosphino-polycarboxylic acid modified inhibitor nanomaterial for oilfield scale control: Synthesis, characterization and migration, *Journal of Industrial and Engineering Chemistry*, Vol. 45, pp 366–374, Jan. 2017, https://doi.org/10.1016/j.jiec.2016.10.004.
27. M. F. Mady, S. Fevang, and M. A. Kelland, Study of Novel Aromatic Aminomethylenephosphonates as Oilfield Scale Inhibitors, *Energy Fuels*, Vol. 33, No. 1, pp 228–237, Jan. 2019, https://doi.org/10.1021/acs.energyfuels.8b03531.
28. I. T. Ismayilov, Anti-Corrosion Ability of Some Surfactants Based on Corn Oil and Monoethanolamine, *AJAC*, Vol. 1, No. 5, pp 79–86, 2013, https://doi.org/10.11648/j.ajac.20130105.11.
29. H. M. Abd El-Lateef, V. M. Abbasov, L. I. Aliyeva, and I. T. Ismayilov, Application of Some Surfactants Based on Corn Oil as Corrosion Inhibitors for Carbon Steel in CO_2 Environments, in *CORROSION 2013*, Orlando, FL: NACE International, Mar. 2013, pp 1–10. https://doi.org/10.5006/C2013-02129.
30. Z. Shen, J. Li, K. Xu, L. Ding, and H. Ren, The effect of synthesized hydrolyzed polymaleic anhydride (HPMA) on the crystal of calcium carbonate, *Desalination*, Vol. 284, pp 238–244, Jan. 2012, https://doi.org/10.1016/j.desal.2011.09.005.
31. K. Popov, M. Oshchepkov, S. Kamagurov, S. Tkachenko, J. Dikareva, and G. Rudakova, Synthesis and properties of novel fluorescent-tagged polyacrylate-based scale inhibitors, *Journal of Applied Polymer Sci*, Vol. 134, No. 26, app.45017, Jul. 2017, https://doi.org/10.1002/app.45017.
32. Y. Xiong and M. Cao, Application of surfactants in corrosion inhibition of metals, *Current Opinion in Colloid & Interface Science*, Vol. 73, 101830, Oct. 2024, https://doi.org/10.1016/j.cocis.2024.101830.
33. Zahraa A. Jawad and Falah K. Matloub, Synergistic corrosion inhibition of carbon steel in cooling tower systems using sodium benzoate, zinc sulfate, and EDTA, *Appl. Chem. Eng.*, Vol. 8, No. 3, 5735, Sep. 2025, https://doi.org/10.59429/ace.v8i3.5735.
34. A. Shaban *et al.*, Synergistic effect of sodium benzoate and EDTA as corrosion inhibitors for carbon steel in chloride-containing solutions, *Corrosion Science*, Vol. 125, pp 61–69, 2017, https://doi.org/10.1016/j.corsci.2017.06.027.
35. N. Brixi, L. Sail, A. Bezzar, O. Sebouai, and S. Benmesmoudi, Temperature Effects on Corrosion Inhibition of Mild Steel in 3% NaCl Solution by EDTA and Sodium Benzoate, in *Proceedings of the Third International Symposium on Materials and Sustainable Development*, B. Abdelbaki, B. Safi, and M. Saidi, Eds, Cham: Springer International Publishing, 2018, pp 385–397. https://doi.org/10.1007/978-3-319-89707-3_45.
36. B. S. Bageri, M. A. Mahmoud, R. A. Shawabkeh, S. H. Al-Mutairi, and A. Abdulraheem, Toward a complete removal of barite (barium sulfate $BaSO_4$) scale using chelating agents and catalysts, *Arab J Sci Eng*, Vol. 42, No. 4, pp 1667–1674, Apr. 2017, https://doi.org/10.1007/s13369-017-2417-2.
37. S. Ziegenheim *et al.*, EDTA analogues – unconventional inhibitors of gypsum precipitation, *Journal of Molecular Structure*, Vol. 1256, 132491, May 2022, https://doi.org/10.1016/j.molstruc.2022.132491.
38. T. Almubarak, J. H. Ng, R. Ramanathan, and H. A. Nasr-El-Din, Chelating agents for oilfield stimulation: Lessons learned and future outlook, *Journal of Petroleum Science and Engineering*, Vol. 205, 108832, Oct. 2021, https://doi.org/10.1016/j.petrol.2021.108832.

39. A. Khormali and D. G. Petrakov, Laboratory investigation of a new scale inhibitor for preventing calcium carbonate precipitation in oil reservoirs and production equipment, *Pet. Sci.*, Vol. 13, No. 2, pp 320–327, May 2016, https://doi.org/10.1007/s12182-016-0085-6.
40. M. Mpelwa and S.-F. Tang, State of the art of synthetic threshold scale inhibitors for mineral scaling in the petroleum industry: a review, *Pet. Sci.*, Vol. 16, No. 4, pp 830–849, Aug. 2019, https://doi.org/10.1007/s12182-019-0299-5.
41. A. T. Kan, Z. Dai, and M. B. Tomson, The state of the art in scale inhibitor squeeze treatment, *Pet. Sci.*, Vol. 17, No. 6, pp 1579–1601, Dec. 2020, https://doi.org/10.1007/s12182-020-00497-z.
42. M.-L. Zhu, H.-J. Qian, R.-X. Yuan, D.-Y. Zhao, H.-C. Huang, and H.-Y. Wang, EDTA interfacial chelation Ca^{2+} incorporates superhydrophobic coating for scaling inhibition of $CaCO_3$ in petroleum industry, *Pet. Sci.*, Vol. 18, No. 3, pp. 951–961, 2021, https://doi.org/10.1007/s12182-021-00558-x.
43. Q. Qu, S. Jiang, W. Bai, and L. Li, Effect of ethylenediamine tetraacetic acid disodium on the corrosion of cold rolled steel in the presence of benzotriazole in hydrochloric acid, *Electrochimica Acta*, Vol. 52, No. 24, pp 6811–6820, Aug. 2007, https://doi.org/10.1016/j.electacta.2007.04.114.
44. L. R. B. Holzle, D. S. Azambuja, C. M. S. Piatnicki, and G. E. Englert, Corrosion behaviour of aluminium in ethyleneglycol–water electrolytes containing phosphonic acid, *Materials Chemistry and Physics*, Vol. 103, No. 1, pp 59–64, May 2007, https://doi.org/10.1016/j.matchemphys.2007.01.007.
45. G. M. Treacy, A. L. Rudd, and C. B. Breslin, Electrochemical behaviour of aluminium in the presence of EDTA-containing chloride solutions, *Journal of Applied Electrochemistry*, Vol. 30, No. 6, pp 675–683, Jun. 2000, https://doi.org/10.1023/A:1003945214539.
46. R. E. Azooz and S. M. Kamal, Corrosion and Corrosion Inhibition of Mild Steel in Red Sea Water by EDTA, *Journal of Material Sciences & Engineering*, Vol. 8, No. 2, 1000517, 2019, https://www.hilarispublisher.com/open-access/corrosion-and-corrosion-inhibition-of-mild-steel-in-red-sea-water-byedta.pdf, [Accessed: Aug. 25, 2026].
47. R. E. Azooz, EDTA as a corrosion inhibitor for Al in 0.5 M HCl: adsorption, thermodynamic and theoretical study, *J. Electrochem. Sci. Eng.*, Vol. 6, No. 3, pp 235-251, Sep. 2016, https://doi.org/10.5599/jese.300.
48. T. A. Ismayilov *et al.*, Study of salts obtained from the interaction of ethylenediamintetraacetic acid with propylamine and isobutylamine as corrosion inhibitors in H_2S condition, *Processes of Petrochemistry and Oil Refining*, No. Special Issue 1, pp 156–164, 2024, https://doi.org/10.62972/1726-4685.si2024.1.156.
49. I. T. Ismayilov, *et al.*, Investigation of Na^+, K^+ salts of propyl- and isobutylamide derivatives of ethylenediaminetetraacetic acid as biocides in relation to sulfate-reducing bacteria, *Processes of Petrochemistry and Oil Refining*, Vol. 24, No. 3, pp 514–525, 2023, https://doi.org/10.36719/1726-4685/95/514-525.
50. T. A. Ismailov *et al.*, Study of the Na^+ and K^+ salts of ethanolamides of ethylenediaminetetraacetic acid as corrosion and salt precipitation inhibitors, *Processes of Petrochemistry and Oil Refining*, Vol. 26, No. 03, 917–932, 2025, https://doi.org/10.62972/1726-4685.2025.3.917.
51. F. Neese, F. Wennmohs, U. Becker, and C. Riplinger, The ORCA quantum chemistry program package, *The Journal of Chemical Physics*, Vol. 152, No. 22, 224108, Jun. 2020, https://doi.org/10.1063/5.0004608.
52. F. Neese, Software Update: The ORCA Program System—Version 6.0, *Wiley Interdisciplinary Reviews: Computational Molecular Science*, Vol. 15, No. 2, e70019, Mar. 2025, https://doi.org/10.1002/wcms.70019.

53. C. Lee, W. Yang, and R. G. Parr, Development of the Colle-Salvetti correlation-energy formula into a functional of the electron density, *Phys. Rev. B*, Vol. 37, No. 2, pp 785–789, Jan. 1988, https://doi.org/10.1103/PhysRevB.37.785.
54. A. D. Becke, Density-functional thermochemistry. III. The role of exact exchange, *The Journal of Chemical Physics*, Vol. 98, No. 7, pp 5648–5652, Apr. 1993, https://doi.org/10.1063/1.464913.
55. G. A. Petersson and M. A. Al-Laham, A complete basis set model chemistry. II. Open-shell systems and the total energies of the first-row atoms, *The Journal of Chemical Physics*, Vol. 94, No. 9, pp 6081–6090, May 1991, https://doi.org/10.1063/1.460447.
56. E. D. Akpan *et al.*, Coordination compounds as corrosion inhibitors of metals: A review, *Coordination Chemistry Reviews*, Vol. 499, 215503, Jan. 2024, https://doi.org/10.1016/j.ccr.2023.215503.
57. I. Azamian, S. R. Allahkaram, M. Johari, and F. Teymouri, Interfacial interaction study of EDTA with the defect structure of $Fe_{3-\delta}O_4$ passive film in an aggressive alkaline medium based on the lattice theory of point defects, *RSC Adv.*, Vol. 12, No. 6, pp 3524–3541, 2022, https://doi.org/10.1039/D1RA07171H.
58. X. Li, J. Zhang, J. Zhang, D. Li, S. Chang, and Z. Lei, Study on the scale inhibition performance of organic chelating agent aided by surfactants on $CaCO_3$ at high salinity condition, *Tenside Surfactants Detergents*, Vol. 61, No. 2, pp 170–178, Mar. 2024, https://doi.org/10.1515/tsd-2023-2549.
59. A. M. Al-Sabagh, N. M. El Basiony, S. A. Sadeek, and M. A. Migahed, Scale and corrosion inhibition performance of the newly synthesized anionic surfactant in desalination plants: Experimental, and theoretical investigations, *Desalination*, Vol. 437, pp 45–58, Jul. 2018, https://doi.org/10.1016/j.desal.2018.01.036.
60. T. A. Ismayilov, V. M. Abbasov, I. T. Ismayilov, R. M. Farhadova, E. A. Manafov, and Ch. K. Salmanova, Effectiveness of propylamide derivatives of ethylenediaminetetraacetic acid against corrosion and salt deposition problems, *SOCAR Proceedings*, No. 4, pp 158–166, 2025, https://doi.org/10.5510/OGP20250401135.
61. E. Udabe, A. Sommers, M. Forsyth, and D. Mecerreyes, Cation Effect in the Corrosion Inhibition Properties of Coumarate Ionic Liquids and Acrylic UV-Coatings, *Polymers*, Vol. 12, No. 11, 2611, Nov. 2020, https://doi.org/10.3390/polym12112611.
62. I. B. Obot, K. Haruna, and T. A. Saleh, Atomistic Simulation: A Unique and Powerful Computational Tool for Corrosion Inhibition Research, *Arab J Sci Eng*, Vol. 44, No. 1, pp 1–32, Jan. 2019, https://doi.org/10.1007/s13369-018-3605-4.
63. H. Balasooriya, C. Li, and F. Wang, Understanding Steel Corrosion: Surface Chemistry and Defects Explored Through DFT Modelling—A Review, *Processes*, Vol. 13, No. 7, 1971, Jun. 2025, https://doi.org/10.3390/pr13071971.
64. H. Lgaz, A. Chaouiki, R. Lamouri, R. Salghi, and H.-S. Lee, Computational Methods of Corrosion Inhibition Assessment, in *ACS Symposium Series*, Vol. 1403, C. M. Hussain and C. Verma, Eds, Washington, DC: American Chemical Society, 2021, pp 87–109. https://doi.org/10.1021/bk-2021-1403.ch006.
65. J. M. Castillo-Robles, E. De Freitas Martins, P. Ordejón, and I. Cole, Molecular modeling applied to corrosion inhibition: a critical review, *npj Mater Degrad*, Vol. 8, No. 1, 72, Jul. 2024, https://doi.org/10.1038/s41529-024-00478-2.
66. S. J. H. M. Jessima, S. S., A. Berisha, A. Oral, and S. S. Srikandan, Corrosion mitigation performance of disodium EDTA functionalized chitosan biomacromolecule - Experimental and theoretical approach, *International Journal of Biological Macromolecules*, Vol. 178, pp 477–491, May 2021, https://doi.org/10.1016/j.ijbiomac.2021.02.166.
67. I. Lukovts, E. Kálmán, and F. Zucchi, Corrosion Inhibitors—Correlation Between Electronic Structure and Efficiency, *Corrosion*, Vol. 57, No. 1, pp 3–8, Jan. 2001, https://doi.org/10.5006/1.3290328.

68. H. Ju, L. Ding, C. Sun, and J. Chen, Quantum Chemical Study on the Corrosion Inhibition of Some Oxadiazoles, *Advances in Materials Science and Engineering*, 519606, 2015, https://doi.org/10.1155/2015/519606.
69. N. S. Orujova *et al.*, In vitro, in silico, and DFT evaluation of antimicrobial imidazole derivatives with insights into mechanism of action, *Sci Rep*, Vol. 15, No. 1, 37723, Oct. 2025, https://doi.org/10.1038/s41598-025-24847-2.
70. M. A. A. Ibrahim *et al.*, Density functional theory study of the corrosion inhibition performance of 6-mercaptopurine and 6-thioguanine expired drugs toward the aluminium (111) surface, *RSC Adv.*, Vol. 13, No. 41, pp 29023–29034, 2023, https://doi.org/10.1039/D3RA04954J.
71. H. M. Abd El-Lateef, V. M. Abbasov, L. I. Aliyeva, E. E. Qasimov, and I. T. Ismayilov, Inhibition of carbon steel corrosion in CO_2-saturated brine using some newly surfactants based on palm oil: Experimental and theoretical investigations, *Materials Chemistry and Physics*, Vol. 142, No. 2–3, pp 502–512, Nov. 2013, https://doi.org/10.1016/j.matchemphys.2013.07.044.
72. A. M. Mammadov *et al.*, Inhibitory-Bactericidal Properties of Phenyldiazenylphenyl-Containing Phenanthroimidazoles and DFT Calculations, *Bulletin of the Russian Academy of Sciences: Physics*, Vol. 89, No. 9, pp 1619–1625, Sep. 2025, https://doi.org/10.1134/S1062873825712322.



Paper submitted: 03.02.2026
Paper revised: 18.07.2026
Paper accepted: 23.07.2026